

# **7 DEVELOPMENT OF A PROTOTYPE SAM RECEIVER**

## **7.1 Introduction**

The feasibility studies described in Chapters 5 and 6 demonstrated the practicality of the SAM field procedure and the efficacy of its signal separation techniques. The potential of SAM to be an efficient, cost-effective, high definition exploration tool was confirmed. The encouragement derived from the success of the feasibility studies justified the initiation of the third and final phase of this project: the development and field-testing of a purpose-designed SAM receiver.

The feasibility trials provided information from which the desirable attributes of a SAM receiver could be specified. Those specifications were realised in the form of a prototype purpose-built option card, the "SAMCard", which interfaces directly to the standard address bus of the TM-4. The SAMCard, TM-4 operating software enhancements and ancillary equipment were designed to the author's specification by GRI electronics engineers, Mr R.C. Bradbury and Mr D.J. McCarthy.

In this chapter, the requirements of a SAM receiver are described along with the strategies employed to accommodate them.

## 7.2 Specifications of a Sub-Audio Magnetics Receiver

The sensitivity and sample rate requirements of a SAM receiver were derived from the feasibility trials. As far as could be determined, the signal from the caesium vapour, optically-pumped magnetic sensor was confirmed to have the appropriate characteristics of dynamic range, sensitivity and frequency response. The signal processing requirements for separating the spatially-varying magnetic field from the synthetically induced modulation then determined the design of the prototype SAM receiver. The requirements of each application were different and it was necessary that the prototype adequately fulfil both functions.

### 7.2.1 Requirements for the Determination of the Spatially-varying Magnetic Field, $H_S$

- (i). **Dynamic Range.** The dynamic range of the spatially-varying magnetic field lies between 20,000 and 80,000 nT.
- (ii). **Sensitivity.** In hand-carried applications, magnetic noise due to mineralisation at the soil/air interface limits the useable sensitivity to 1 or 0.1 nT in most localities. In airborne applications, interference from the aircraft usually limits the useable sensitivity to 0.1 or 0.01 nT.
- (iii). **Sample Rate.**  $H_S$  is required to be sampled at intervals no greater than one elevation unit above ground. At normal airborne and hand-held survey speeds, this requirement can usually be met with sample rates between 5 and 10 per second. However, the need to remove the SAM modulation or interference from mains power noise or rotating aircraft components is best met using real-time digital filters, processing data sampled at twice the highest frequency present in the noise. A sample rate of the order of 200 samples per second is required for this purpose.

### 7.2.2 Requirements for the Determination of the SAM Signal, $H_{Mod}$

- (i). **Precision.** With SAM signal amplitudes of just a few nanotesla, the desired measurement resolution is in the order of pT. However, given the potential to use

digital signal enhancement techniques, resolution down to tens of pT is considered adequate.

- (ii). **Bandwidth.** A bandwidth of 0 to 500 Hz was specified. Transmitted square wave signals in the sub-audio frequency range may then be received without distortion of the significant higher harmonics.
- (iii). **Constant Sample Interval.** Constant sample interval is required so that essential statistical noise reduction can be performed.
- (iv). **Synchronisation with the Transmitter.** Precise synchronisation with the transmitted signal is required due to the need to detect polarity reversals in the received signal and to quantify phase lags between the received signal and the transmitted signal.
- (v). **Real-time Separation of  $H_{Mod}$  and  $H_S$ .** A high pass filter is required with a roll-off of at least 24 dB/octave and cutoff frequency in the range of 1-5 Hz such that the chosen fundamental frequency of  $H_{Mod}$  may be passed unaffected, is required to extract  $H_{Mod}$  from  $H_T$ . A complementary lowpass filter in the same frequency range is required to extract  $H_S$  from  $H_T$ . These filters are a fundamental requirement if the receiver is to separate, in real-time, the SAM modulation,  $H_{Mod}$ , from the low frequency variation due to the spatially-varying magnetic field,  $H_S$ .
- (vi). **Real-Time Removal of Mains Power Interference.** An optional, digital 50/60 Hz notch filter is required to remove interference from mains power in localities where this exists.
- (vii). **Sample Rate.** Experience from the feasibility trials indicated that in the absence of conductors extending to the ground surface, the TFMMR and “probably” the TFMMIP measurements need to be acquired at sample intervals no closer than two to five elevation units. At normal hand-held and airborne survey speeds, this requirement can usually be met with sample rates of 0.2 to 1.0 per second.
- (viii). **Sampling Frequency must be a multiple of the Transmitter Frequency.** To facilitate averaging of the recorded waveforms without resorting to interpolation, the sampling frequency must be a multiple of the transmitter frequency. This is commonly achieved by using transmitter and sampling frequencies which are

powers of two. As the required bandwidth was nominally 500 Hz, a sample rate of 1024 samples per second (thereby providing a bandwidth of 512 Hz) was considered appropriate.

- (ix). **Real-Time Processing Capability.** Ideally, a SAM receiver would have the ability to perform real-time spectral analysis and/or integration of time domain decays in order to determine parameters characterising the received signal.

## 7.3 The Approach Used

While the TM-4 already meets some of the defined specifications, other attributes were found to be unsuitable for the tasks required of a SAM receiver. In particular, the TM-4 was designed with a period counter specifically to obtain high measurement resolution at fast sample rates. If the receiver is to be capable of measuring TFMMR and TFMMIP parameters, a high resolution, constant sample interval counter, capable of being synchronised with the transmitter, is demanded. From a technical perspective, the requirements for both high bandwidth and high measurement resolution are antagonistic. If SAM were to achieve its full potential, this problem had to be overcome.

The approach taken in the prototype receiver was to implement parallel processing streams, each designed to meet a particular specification. One processing stream was designed to obtain the spatially-varying magnetic field measurements; the other to extract the SAM signal parameters. Although the strategies employed were to eventually encompass the use of different transmitter frequencies, the initial development assumed a transmitter frequency of 8 Hz. The techniques used are described by Bradbury (1994a) and Cattach *et al.* (1995b) and are summarised below.

### 7.3.1 Total Magnetic Field Measurements

In order to determine the spatial geomagnetic field variation, the Larmor signal is fed into the standard TM-4 period counter. Real-time digital filtering is then applied to the data to remove the high frequency component due to the SAM signal. For an 8 Hz

transmitted signal, the filter employed is a 41-point Finite Impulse Response Lowpass digital filter providing an attenuation of >40 dB at 6 Hz and above.

### **7.3.2 The SAM Measurements - The SAMCard**

In order to process the SAM signal, a purpose-built option card was constructed. The “SAMCard” interfaces directly to the address bus in the TM-4 and is responsible for recovering and preparing the SAM signal for subsequent digital signal processing procedures. The input to the SAMCard is a 5 V logic signal varying at the Larmor frequency. The SAM signal appears as frequency modulation of the Larmor frequency. A schematic describing the functionality of the SAMCard is shown in Figure 7-1.

#### ***7.3.2.1 The Demodulation Circuit***

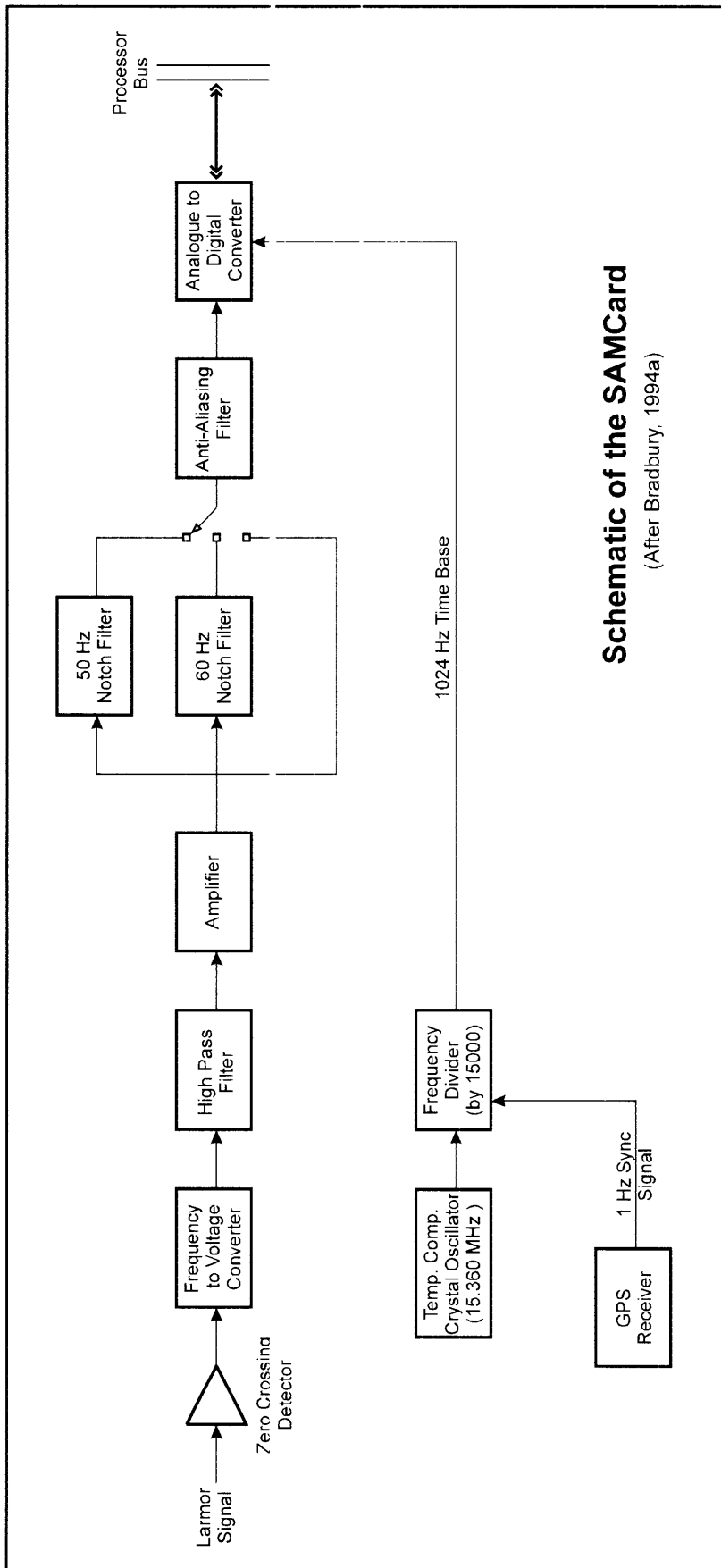
The Larmor signal is “squared up” and input to a frequency to voltage converter which serves to “back off” the high amplitude DC component due to the earth’s ambient magnetic field ( $\approx 50,000$  nT). The result is an output voltage which is modulated by the SAM signal.

#### ***7.3.2.2 Removal of Low Frequency Noise***

The demodulated signal is then high pass filtered to separate the SAM signal,  $H_{Mod}$ , from that due to the earth’s spatially-varying magnetic field,  $H_S$ . The filter also provides carrier suppression which would otherwise overload the following stages.

#### ***7.3.2.3 Anti-Aliasing Filter***

In order to provide a flat response from the frequency of the transmitted signal to the Nyquist frequency of about 500 Hz, an anti-aliasing filter was incorporated into the circuit. High frequency roll-off was provided by a 4-pole Butterworth filter implemented as 2x2-pole Sallen-Key filters. The filter has a cutoff frequency of 482 Hz and a roll-off of 24 dB per octave.



**Schematic of the SAMCard**  
(After Bradbury, 1994a)

Figure 7-1. Schematic of the SAMCard (After Bradbury, 1994a).

#### ***7.3.2.4 Mains Power Filters***

An optional mains power frequency notch filter was also provided. This filter is switchable between 50/60 Hz. The filter is implemented as a bootstrapped (positive feedback) twin-T R-C filter which provides a deep notch at a single frequency.

#### ***7.3.2.5 Analogue to Digital Conversion***

Digitisation of the analogue signal was accomplished with the aid of a 13-bit A to D converter. Timing of the A to D converter is governed by a 15.360 MHz temperature-compensated crystal oscillator. The output of the oscillator is frequency divided to provide a 1024 Hz time base. The output of the A to D converter is amplitude scaled to 0.043 nT per least significant bit providing a range of +/- 150 nT.

#### ***7.3.2.6 Transmitter - Receiver Synchronisation***

As described by Dodds (1981), several techniques have been employed to synchronise IP transmitters and receivers. These include hard-wire links, radio links and temperature-stabilised crystal oscillators. Each of these techniques poses problems in the field. Hard-wire links are impractical for a moving system. Radio links lack reliability and often require licenses which means that they may not be useable in all locations. The disadvantages of temperature-stabilised crystal oscillators for use in portable systems include the power consumption required for the temperature-controlled ovens and the complexity of the circuitry required to achieve synchronisation. Logistical disadvantages include the requirement to bring the instruments together for synchronisation. An innovative solution to these problems was provided by the use of GPS time.

The synchronisation technique adopted for the prototype SAM system employs Trimble SVeeSix GPS receivers to provide accurate timing strobes to both the SAM receiver and a purpose-built transmitter controller (the "SAM-XMT" - described in Section 7.5). The SVeeSix is a low-cost, lightweight, high performance GPS receiver board set which is designed specifically for OEM's and system integrators. The board uses six channels to track up to eight satellites, automatically selecting the optimum satellite combination

for obtaining the most accurate position solution. The unit is described in detail by Trimble Navigation Limited (1992)

In addition to the standard positional data information, the SVeeSix provides a one microsecond pulse-per-second output. The falling edge of the pulse is synchronised with Universal Coordinated Time (UTC). The timing accuracy is  $\pm 1 \mu\text{s}$  and is valid when computing position fixes from multiple satellites as well as when using the system's static, one satellite, time-only mode. The SVeeSix units are fitted with RS-232 connectors which enable configuration and monitoring of the output with a computer. The antenna units consist of a 60 mm diameter low profile patch antenna element. The SVeeSix unit is small enough to be mounted inside the TM-4 casing. Power is supplied directly from the TM-4. The 1 Hz synchronisation signal is input to the frequency divider which resets the 1024 Hz time base. Synchronisation is such that the A to D converter will digitize its first value 0.78 ms after receiving the GPS pulse.

The main advantage of the GPS synchronisation technique is that the system dynamically updates the crystal oscillators in both the transmitter and receiver from an independent and very precise timing source. Consequently, drift of the oscillators is generally contained within one second periods.

The only disadvantage of GPS synchronisation is that in forested areas, it is difficult to maintain satellite lock due to interference from the tree canopy. For this reason the transmitter should be located in an available clearing. If satellite lock is lost by the GPS unit in the SAM receiver, synchronisation becomes dependent on the stability of the GPS unit's internal crystal oscillator. To minimise the effect of this, it may, in such circumstances, become necessary for the operator to return to a cleared area from time to time if quality phase measurement is to be maintained.

Sources of synchronisation error include:

- The timing accuracy of the GPS pulse-per-second is  $\pm 1 \mu\text{s}$  for the receivers in both the SAMCard and the SAM-XMT transmitter controller.
- The accuracy of resetting the crystal oscillators. For the SAMCard:  $\pm 0.5$  cycles of the 15.36 MHz reference clock:  $\pm 0.03 \mu\text{s}$ . For the SAM-XMT:  $\pm 2.0$  cycles of the 15.36 MHz reference clock:  $\pm 0.13 \mu\text{s}$ .



- The maximum drift of the crystal oscillators used in the SAMCard and the SAM-XMT over a one second period is  $\pm 1 \mu\text{s}$  for both instruments.

The estimated worst case synchronisation accuracy, assuming satellite lock is not lost, is  $\sim 5 \mu\text{s}$ . Calculation of the phase error due to the time error between two time references is described by Frangos (1990) and may be calculated as follows:

$$\phi_{Error} = \frac{2\pi t_{Error}}{T} \quad \text{Eqn 7-1}$$

where  $t_{Error}$  = the time difference between the references, and  
 $T$  = the period of the waveform

Consequently, a  $5 \mu\text{s}$  discrepancy between the transmitter and receiver clocks will produce a 0.25 mrad phase error at 8 Hz. With expected phase lags due to induced polarisation effects of say, 10 to 50 mrad, this error was considered acceptable. However, if satellite lock is lost due to the mobile receiver passing beneath tree canopy, a maximum drift error of  $\pm 1 \mu\text{s/s}$  (0.05 mrad/s at 8 Hz) may occur until satellite lock is regained and synchronisation is once again achieved.

At this drift rate, loss of satellite lock for a period of one minute would result in a maximum phase error of 3 mrad. In areas where trees are sparse, satellite lock is typically lost for no more than 10- 5 s when traversing at walking speed. Clearly, the technique would not be suitable for hand-held surveys in localities with dense tree cover.

## 7.4 TM-4 Enhancements

A desirable requirement for the SAM receiver is the capability to process the received waveforms in real-time. However, during the development of the prototype SAM receiver, it was considered more appropriate to record the raw data for post processing rather than to attempt processing the signals in real-time. The philosophy behind this decision was the perceived requirement for a research platform from which it would be possible to measure and assess any deficiencies in the system. By so doing, processing

strategies may be refined, before becoming committed to a less flexible, embedded system.

The TM-4 operating system software required major modification. This included the incorporation of the following facilities:

- (i). **Recording of Entire Waveforms.** In order to enable spectral analysis of the raw data, the entire SAM waveform was required to be recorded at the rate of 1024 measurements per second whilst also recording the spatial magnetic field at preset measurement distance intervals.
- (ii). **Waveform Averaging (Stacking).** The TM-4 was made capable of stacking the SAM data over preselectable window widths prior to recording. This has the advantage of improving the signal-to-noise ratio whilst reducing the volume of the data to be recorded. Typically, for an 8 Hz waveform, the data would be stacked for eight cycles resulting in a single averaged waveform per second. At walking speed, this would translate to a single recorded waveform per 1.5 m of traverse. Stacking over longer periods would further reduce noise levels but at the expense of spatial resolution. Figure 7-2 illustrates an unstacked “noise only” signal recorded with the SAMCard together with its amplitude spectrum. The effect of stacking on incoherent noise is to reduce the RMS noise level by a factor of  $1/\sqrt{N}$ , where  $N$  is the number of periods of the waveform averaged (Dodds, 1981). The result of stacking eight periods of the waveform in Figure 7-2 is shown in Figure 7-3 where the 1/3 noise reduction is evident.
- (iii). **Binary Recording Format.** This option was included to enable more efficient use of available memory.
- (iv). **High Speed Data Transfer.** Because of the large volume of data recorded by the system, the data transfer rate was increased from 9600 baud to 19200 baud.

Apart from the addition of the SAMCard, hardware modifications included a redesign of the TM-4 CPU board to increase memory capacity to 6 MB and to increase the speed of the CPU from 12 MHz to 16 MHz. Other modifications included the Trimble SVeeSix GPS interface. For the prototype receiver, the SVeeSix was mounted on the TM-4's carry harness (see Plate 7-1).

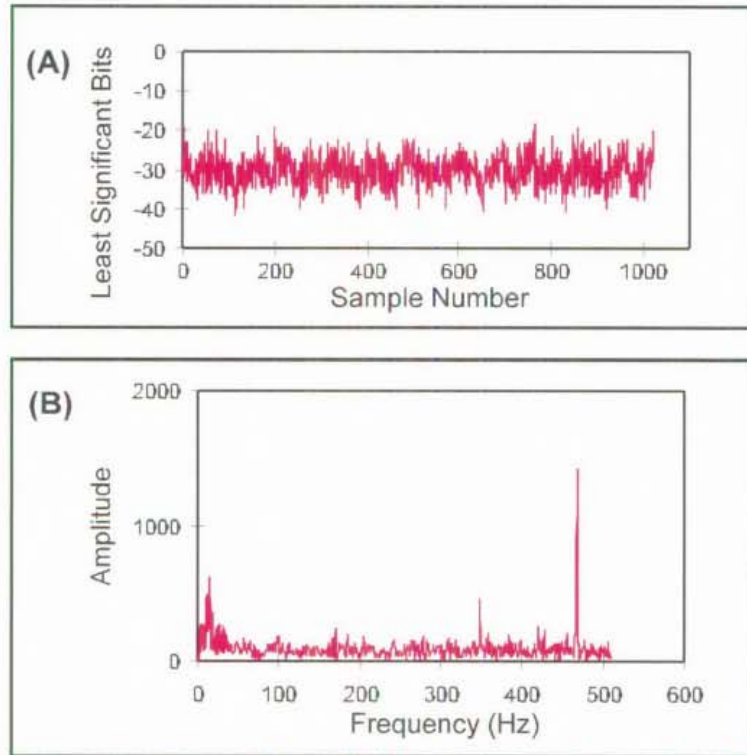


Figure 7-2. (A) Unstacked, 1024 point waveform recorded from the SAM signal simulator without SAM modulation, and (B) The amplitude spectrum of the waveform in (A) (After Bradbury, 1994a).

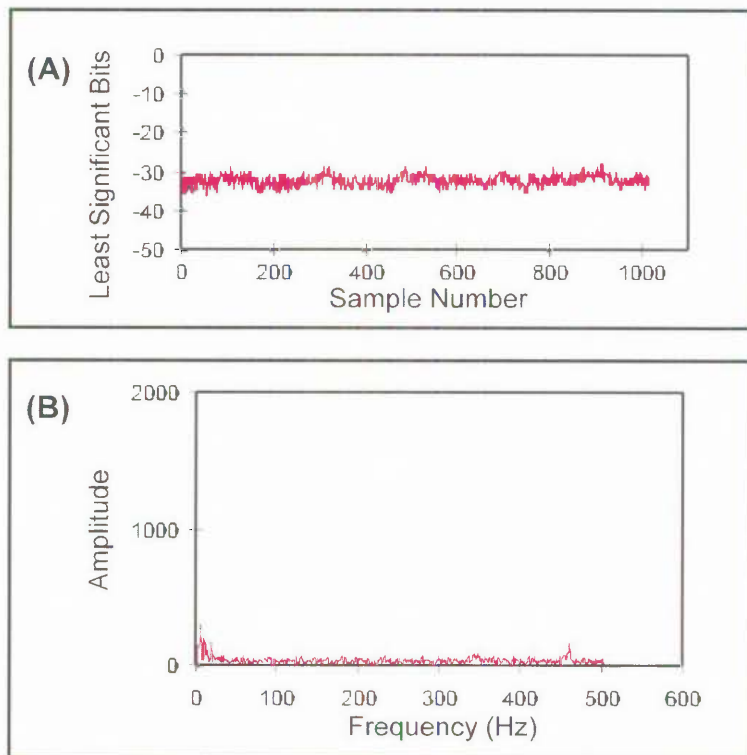


Figure 7-3. (A) Stacked, 1024 point waveform recorded from the SAM signal simulator without SAM modulation, showing the effect of 8x stacking, and (B) The amplitude spectrum of the waveform in (A) (After Bradbury, 1994a).

## 7.5 The SAM-XMT Transmitter Controller

The synchronisation technique used for the SAM system required the development of a transmitter controller. The SAM-XMT is a waveform generator, the specifications of which are summarised in Table 7-1. It incorporates a Trimble SVeeSix GPS unit to provide synchronisation to UTC time and was designed to be compatible with the Zonge series of transmitters. The SAM-XMT controller is depicted in Plate 7-2.

Specifications of the SAM-XMT Transmitter Controller		
<b>Function</b>		
To produce a waveform with which to drive the Zonge series IP/EM transmitters		
To provide waveform synchronisation aligned to GPS 1Hz strobe		
To accept power from external 6 x 6V 4AH battery pack - compatible with TM4 charger		
To have reverse polarity protection		
To supply power to an internal GPS receiver		
<b>Parameters</b>		
Frequencies - switchable	1, 2, 4, 8, 16, 32, 64, 128	Hz
Duty Cycle - switchable	100, 50, 25, 12.5	%
Short term frequency accuracy	±1	ppm max
Battery life between charges	30	hours operation min
<b>Controls</b>		
Power ON/OFF	Toggle switch	
Power Fuse	250	mA
Frequency	Rotary switch	
Duty Cycle	Rotary switch	
<b>Indicators</b>		
Power ON / Battery OK	LED	
GPS Strobe	LED	
<b>Inputs/Outputs</b>		
Zonge transmitter	GND	
CRO monitor GPS STROBE	GND	
CRO monitor POLARITY	GND	
CRO monitor DUTY CYCLE	GND	
External clock input	GND	
Power from TM-4 battery pack	6 x 6V battery input	12V unregulated at 0.25A
GPS antenna - Trimble SV6	GND	Antenna input
GPS serial port	9-pin RS-232 DCE TSIP	Straight through cable

Table 7-1. Specifications of the SAM-XMT Transmitter Controller (After McCarthy, 1994).



Plate 7-1. The TM-4 based SAM Receiver showing the mounting position of the Trimble SVeeSix GPS Receiver.

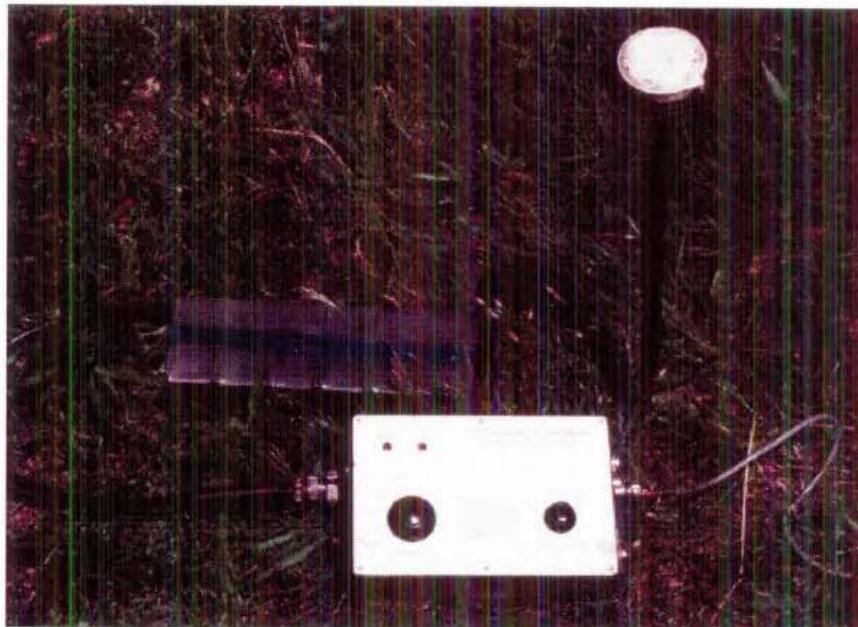


Plate 7-2. The SAM controller incorporating the Trimble SVeeSix GPS Receiver.

## 7.6 The SAM Signal Simulator

The development of the SAMCard electronics required specialised laboratory test equipment. Laboratory testing of magnetometer instrumentation is usually difficult because of uncontrolled fluctuating ambient magnetic fields, a major source of which is mains power. An alternative to using a caesium magnetometer sensor for testing purposes was to use a signal generator to simulate the Larmor frequency produced by a sensor.

A number of available signal generators were tested for this purpose prior to the development of the SAM receiver. However, they were found to be inadequate for the task because of a lack of stability at the required frequencies resulting in an unacceptable level of noise in the SAM bandwidth. Those that were mains powered introduced excessive 50 Hz noise into the generated signal. It was evident that in order to test the performance of the SAMCard, a clean, stable, controllable reference signal, capable of emulating the frequencies, modulation amplitudes and noise characteristics expected from a SAM signal would be required. A SAM signal simulator was, therefore, built for this purpose before development of the SAMCard could continue.

The SAM simulator is a self-contained signal generator which simulates the Larmor signal produced by an alkali vapour magnetometer. The simulator may be connected to the TM-4 in place of the caesium vapour sensor and may be powered from an external DC power source or directly from the TM-4. In the latter case, the load on the TM-4's power supply is equivalent to that due to the sensor.

The Larmor signal is a sinusoidal voltage whose frequency is proportional to the ambient magnetic field intensity. Added to this sine wave is bandwidth-limited white noise. In order to simulate the SAM signal, the output may also be frequency modulated with an internal low frequency square wave or via an external input. A schematic of the SAM Signal generator is shown in Figure 7-4. Its specifications are summarised in Table 7-2.

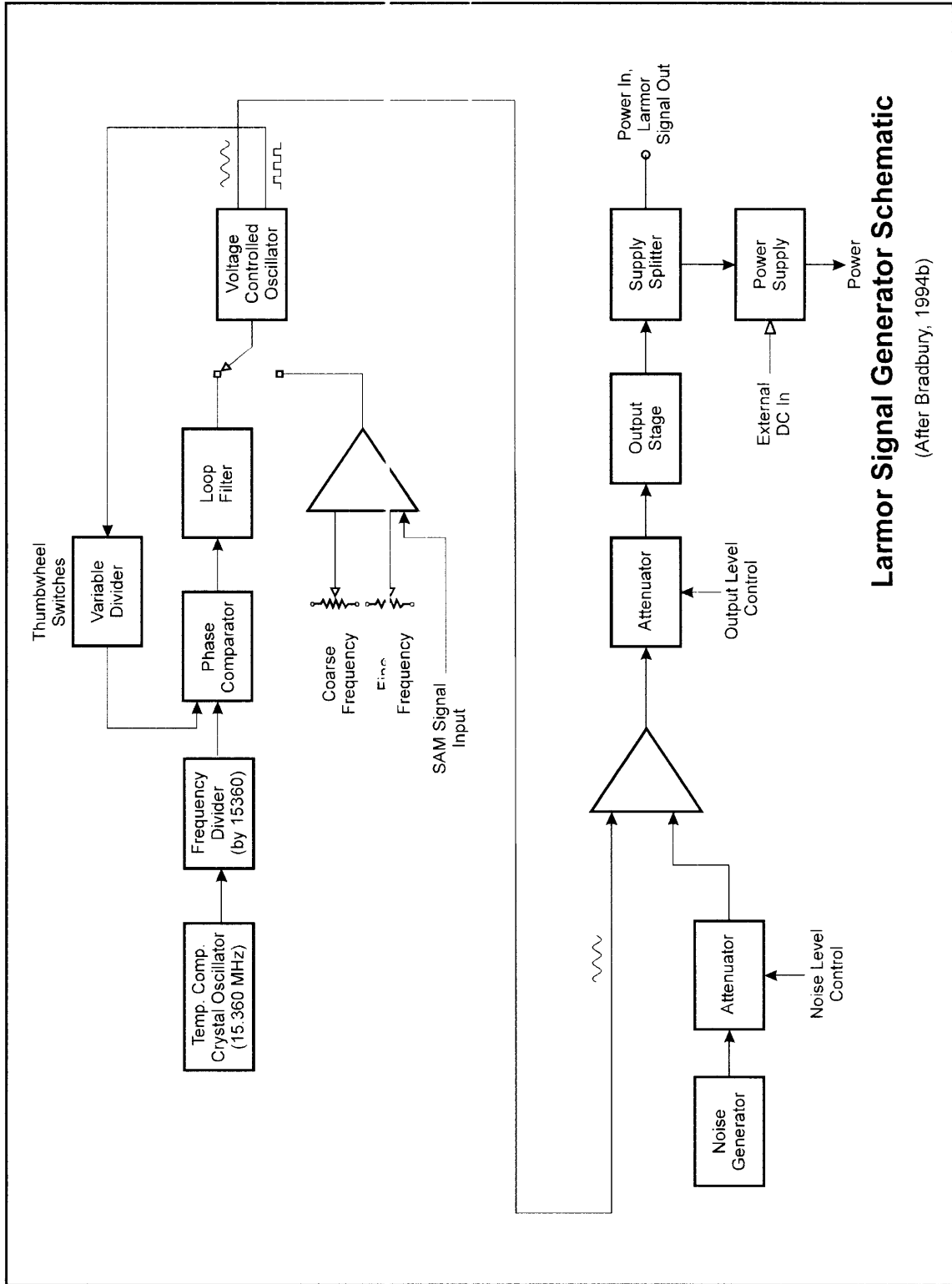


Figure 7-4. Larmor Signal Generator Schematic (After Bradbury, 1994b).

Specifications of the SAM Signal Generator		
<b>Larmor Simulation Output</b>		
Type	sinusoidal voltage with white noise	
Frequency Range	100 - 225	kHz
Frequency Step	1	kHz
Fine Adjustment	± 5	ppm
Equivalent Mag Range (Cs	28,000 - 65,000	nT
Sine Amplitude	0.1; 0.3; 1.0; 3.0	Vp-p
Noise Amplitude	Off -50 -40 -30	dB
Noise Bandwidth	6	MHz
Frequency Reference	Internal; External	
Internal Frequency Accuracy	± 1	ppm
Rated Output Load	1000 Ohms + 100 nF	
Output Impedance	5	Ohms
DC Withstand Voltage	± 50	V
Short Circuit Duration	continuous	
<b>SAM Simulation</b>		
Type	frequency modulation of LARMOR signal	
Modulation Source	Internal; External	
Internal Modulation	8	Hz
Modulation Depth	adjustable with cal position	
Modulation Depth At Cal	10; 100	Hz/Volt
Modulation Bandwidth	5	kHz
<b>Other</b>		
Power Source	TM-4; external supply	
External Supply	+18 - +30 unregulated	V
External Oscillator	TTL	
Auxiliary Outputs	Larmor signal monitor	
Dummy Load	500mA at 30V switchable	

Table 7-2. Specifications of the SAM Signal Simulator (After Bradbury, 1994b).

## 7.7 Data Processing

The PC-based signal processing steps developed for the SAMCard include some of the standard procedures used to process IP data. Exceptions include the need to correct for the frequency response of the SAMCard and to correct for the influence of the Primary field,  $H_{Primary}$ . The steps involved, include the following:



### 7.7.1 Correction for the SAMCard Filter Response

The SAMCard analogue circuitry is characterised by the Amplitude and Phase responses shown in Figure 7-5. The responses shown are for a high pass filter with a cutoff frequency of 6 Hz and a lowpass anti-aliasing filter with a cutoff frequency of 482 Hz.

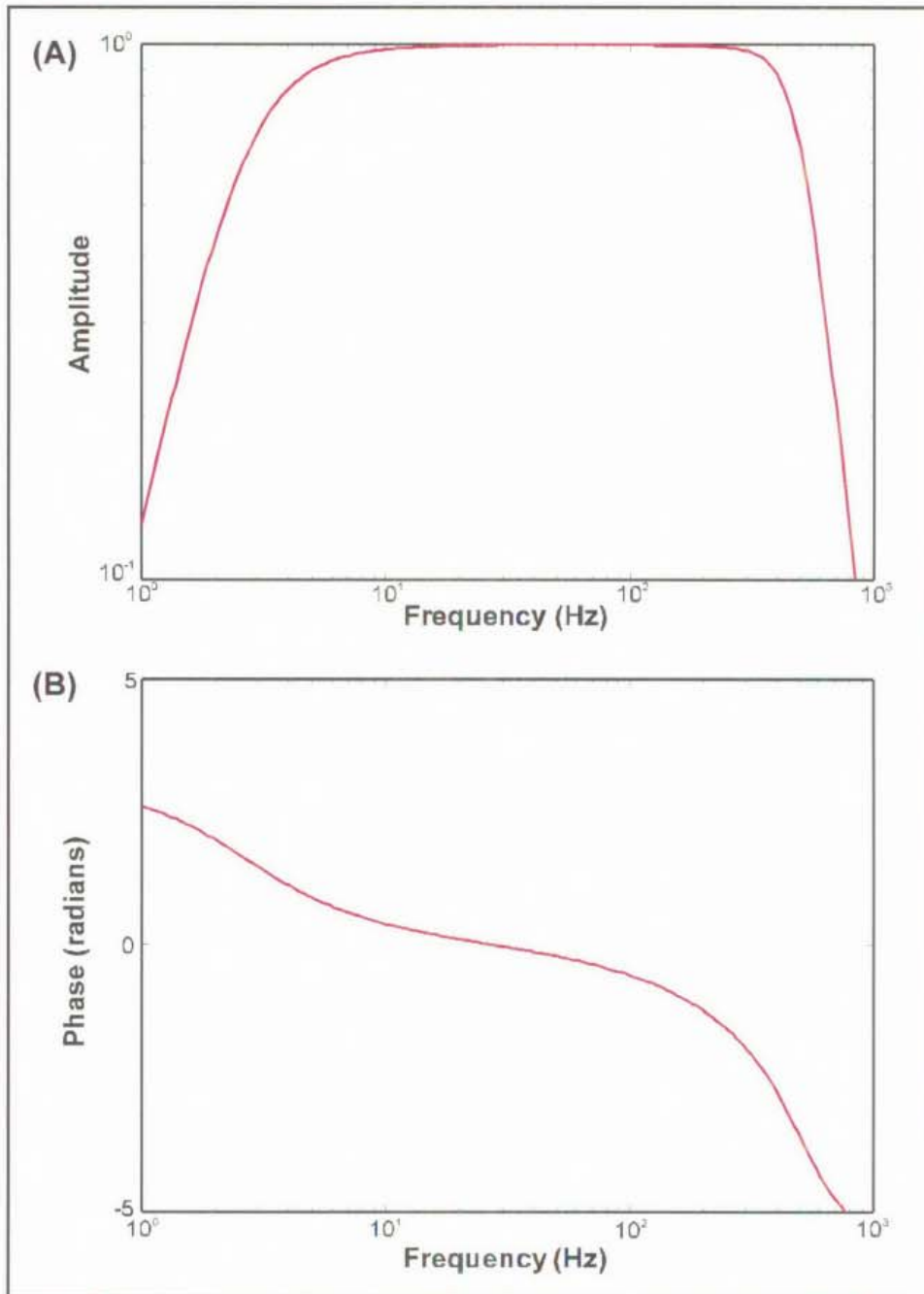


Figure 7-5. (A) Amplitude response, and (B) Phase response of the SAMCard (After Bradbury, 1994a).

The frequency response causes distortion of the SAM signal largely due to the high pass filter not having a perfectly flat response at frequencies above the cutoff frequency (see Figure 7-5(A)). However, the filter response is theoretically fixed and, for calculation of frequency domain parameters, it is not of concern. If time domain parameters are required, the square wave may be corrected by applying a compensating filter to the waveform. Figure 7-6 illustrates the result of applying the compensating filter.

The inverse filter response is based on the theoretical calculation of the transfer function of the demodulation circuit. Initially, the compensation filter coefficients were determined using the nominal circuit component specifications. However, the actual circuit frequency response was found to be slightly different from the nominal values. A more accurate compensation filter was therefore calculated from measurement of the actual frequency response.

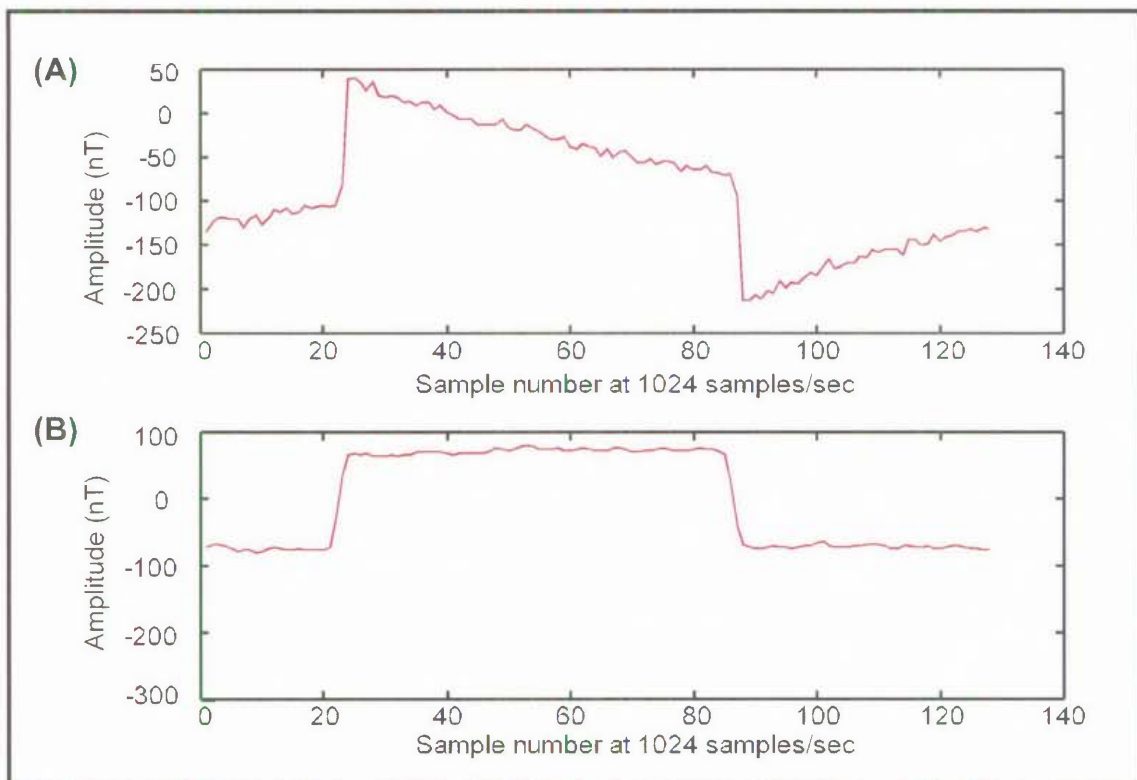


Figure 7-6. (A) Typical SAMCard recording of a square wave produced by the SAM signal generator showing distortion due to the SAMCard's filter response, and (B) The result of correction of the recorded data by applying the compensation filter (After Bradbury, 1994a).

## 7.7.2 Slope correction

The slope correction is analogous to SP slope correction in IP surveys. However, the main component of low frequency noise present in the data is usually the residual spatial magnetic field variation after processing with the high pass filter. If entire waveforms are recorded, slope correction is best achieved by applying a high pass, zero phase, digital filter as used for the feasibility studies. For stacked waveforms, the slope correction is a linear estimate based on the statistical distribution of the data within each waveform.

## 7.7.3 Calculation of parameters

The IP or MIP parameters commonly used are described in Chapter 2. Once the received waveforms have been reconstructed by application of the inverse filter response, any of those standard parameters may be calculated. However, a significant difference does exist in that both TFM MR and TFM MIP parameters must be corrected for the influence of the Primary field  $H_{Primary}$ .

### 7.7.3.1 Corrections for TFM MR Parameters

In both time and frequency domain surveys, the peak amplitude of the SAM modulation,  $H_{pk}$ , can be determined by integrating under the “on” time. Alternatively, the amplitude of the fundamental frequency may be used to determine  $H_{pk}$  as described for the feasibility studies.  $H_{pk}$  consists of both  $H_{Primary}$  and  $H_G$ . Therefore, calculation of  $H_G$  requires calculation and subtraction of  $H_{Primary}$  from  $H_{pk}$ .

The correction of  $H_G$  for the Normal field,  $H_{Normal}$ , may be performed for each data point or performed once the data has been gridded. For the purposes of research, the determination of the Normalised TFM MR anomaly,  $H_N$ , was achieved by subtracting  $H_{Normal}$  from the grid files. The reason for this approach was to enable the examination of the imaged data before and after normalisation so that judgement could be made as to the validity of the process.

### 7.7.3.2 Corrections for TFMMIP Parameters

If time domain waveforms are used, a TFMMIP “chargeability” parameter may be determined by integrating under the decay curves in the “off” time as per conventional IP surveys. Normalisation of the parameter for the strength of the signal must be determined by division by  $H_G$ , not  $H_{Mod}$ .

Calculations of phase relationships must also take into account the fact that  $H_{Mod}$  includes the influence of the Primary field. As an example, the phase relationship between  $H_{Mod}$ ,  $H_{Primary}$  and  $H_G$  is illustrated in Figure 7-7.

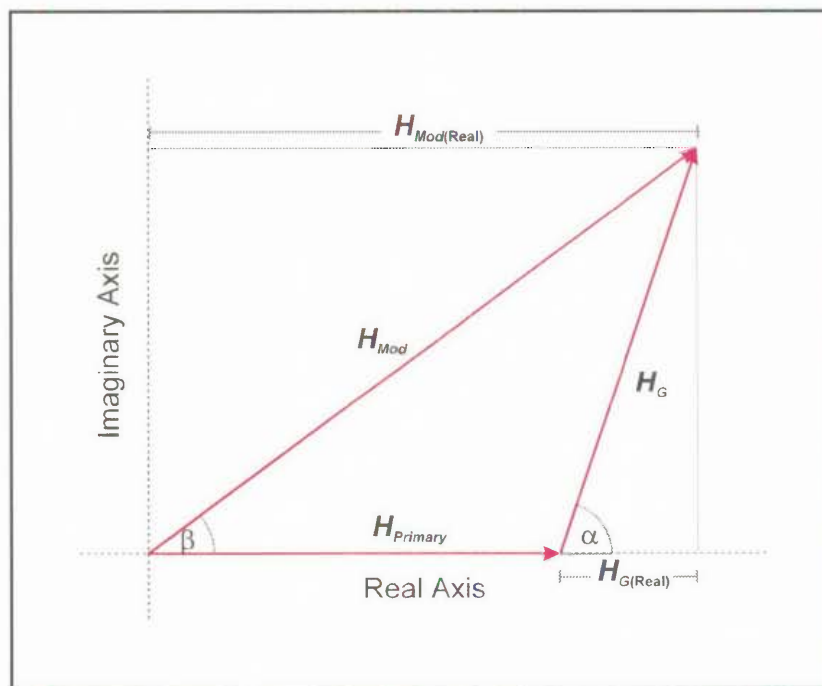


Figure 7-7. Diagram showing the phase relationship between  $H_{Primary}$ ,  $H_G$  and  $H_{Mod}$ .

The received signal, after removal of  $H_S$ , is  $H_{Mod}$ . Calculation of the phase lag of  $H_{Mod}$  with respect to the transmitted current will result in the angle  $\beta$ . The phase lag angle of  $H_G$  with respect to the transmitted current is  $\alpha$ . The first step in determining  $\alpha$  is to find the real component of  $H_{Mod}$  which can be calculated from the trigonometric relationship:

$$|H_{Mod(Real)}| = |H_{Mod}| \cos \beta \quad \text{Eqn 7-2}$$

The real component of  $H_G$ ,  $H_{G(\text{Real})}$  may be determined by subtracting  $H_{\text{Primary}}$  from  $H_{\text{Mod}(\text{Real})}$ . The amplitude of  $H_G$  is known and  $\alpha$  may then be solved as follows:

$$\alpha = \cos^{-1} \left( \frac{|H_{G(\text{Real})}|}{|H_G|} \right) \quad \text{Eqn 7-3}$$

The software must also take into account the fact that polarity reversals (see Chapter 5) do occur and that  $H_G$  may be  $180^\circ$  out of phase from  $H_{\text{Primary}}$ .

#### 7.7.4 Conclusion

The development of the prototype SAMCard was a first attempt to address the problem that the SAM specification developed from the feasibility trials contained an incompatibility with existing instrumentation, that is, the required counter resolution and sample rates were not attainable with the existing period counter technology. The development of the prototype SAMCard provided a solution for achieving those specifications. A series of field tests were performed using the SAMCard technology to enable an assessment of the strategies employed. The results of these studies are presented in Chapter 8.